

# Improvement of Saturation Magnetization of Sputtered Fe/Al Multilayer Thin Films Using Taguchi Method Supported by ANOVA, Response Surface Methodology and Regression Analysis

H. KÖÇKAR<sup>a,\*</sup>, N. KAPLAN<sup>a</sup>, A. KARPUZ<sup>b</sup> AND O. KARAAGAC<sup>a</sup>

<sup>a</sup>Balikesir University, Science and Literature Faculty, Physics Department, 10145, Cagis, Balikesir, Turkey

<sup>b</sup>Karamanoglu Mehmetbey University, Kamil Ozdag Science Faculty, Physics Department, Karaman, Turkey

Received: 02.02.2023 & Accepted: 02.03.2023

Doi: [10.12693/APhysPolA.143.381](https://doi.org/10.12693/APhysPolA.143.381)

\*e-mail: [hkockar@balikesir.edu.tr](mailto:hkockar@balikesir.edu.tr)

Taguchi method has been conducted to improve the saturation magnetisation,  $M_s$ , of Fe/Al multilayer thin films deposited using a dual-target magnetron sputtering. The  $M_s$  values were obtained from the magnetic hysteresis loops. To evaluate the influence of deposition factors on  $M_s$  by using the Taguchi method, L9 orthogonal array with three deposition factors (A — Fe deposition rate, B — Al deposition rate, and C — Fe layer thickness) was carried out with nine experiments at three levels. For the signal-to-noise ratio of the “larger is the better”, the improved  $M_s$  has been obtained at A3B2C3, where factor A is 0.12 nm/s, factor B is 0.03 nm/s, and factor C is 25 nm. At A3B2C3, a verification experiment was carried out with a 95% confidence level to confirm the prediction of 1597.6 emu/cm<sup>3</sup>, and in the experimental run,  $M_{s, \text{exp}}$  was found to be 1649.0 emu/cm<sup>3</sup>, which was an improvement from the highest initial run, i.e.,  $M_{s, \text{ini}} = 1540.2$  emu/cm<sup>3</sup>, among prescribed runs. Analysis of variance was imposed to obtain the F-ratio and contribution percentage of each deposition factor. Also, the interactions of the deposition factors were determined with response surface methodology. For the structural properties at the best factor combinations, X-ray diffraction experiments revealed that Fe/Al films at A3B2C3 were crystallised with the mixed phase of face-centred cubic and body-centred cubic structures. According to scanning electron microscope images, the film surface is almost uniformly shaped. Furthermore, the model of  $M_s$  has also been developed using regression analysis as a function of the deposition factors A, B, and C. Then, from the regression model, high statistical performance was obtained, with values of  $R^2$  and  $R^2(\text{adj})$  being 100 and 100%, respectively. It is seen that the Taguchi method supported by response surface methodology, analysis of variance, and regression analysis turned out to be very successful in finding the factors with proper levels in order to improve  $M_s$  of Fe/Al multilayer thin films within the prescribed limit.

topics: Fe/Al multilayer thin films, Taguchi method, response surface method, regression analysis

## 1. Introduction

The importance of magnetic films in today's science and technology has been proven by many studies [1–4]. These films are produced with different production techniques [5–7], including the sputtering method [8, 9]. Among the studies of magnetic films [7, 9, 10], there is a large number of investigations of Fe-containing structures. There are many studies in which Fe is used together with Al to form different types of structures and in which their various properties are examined [11, 12]. Fe/Al multilayers are an important type of these structures [13, 14]. In [13], Fe/Al multilayers were produced by changing each parameter and keeping the order of the rest of the parameters constant, i.e., using the “one factor at a time” method. These param-

eters are Al layer thicknesses (7.5, 35, and 95 nm), Al deposition rates (0.02 and 0.06 nm/s), Fe layer thicknesses (7.5, 12.5, and 27.5 nm), and total film thicknesses (100, 125, and 175 nm). Researchers also focused on the low-temperature noncollinear magnetic behaviour in ultrathin Fe/Al multilayers [14]. It is important to obtain multilayer thin films (MTFs) with required properties that are key to potential magnetic applications. In this sense, as a technique, Taguchi design is a very handy method in large areas [15–21] to obtain the desired properties. Kamaruddin et al. [15] used the Taguchi method for the optimization of injection moulding parameters for plastic blend production. Another study was done by Rama and Padmanabhan [16], where the Taguchi method was used for setting the parameters of the electrochemical

TABLE I

Deposition factors, their symbols and level settings.

Deposition factor	Symbol	Level 1 (Low)	Level 2 (Medium)	Level 3 (High)
Fe deposition rate [nm/s]	A	0.02	0.07	0.12
Al deposition rate [nm/s]	B	0.02	0.03	0.04
Fe layer thickness [nm]	C	5	15	25

machining process of Al/5%SiC composites. The method was also used to enhance the process parameters of the drilling of EN 31 steel in study [17]. Also, Taguchi's method was applied to improve the surface finish characteristics of faced components in drilling operation [18]. In addition, the Taguchi method was used to successfully optimize parameters for adhesion strength of sputtered Ti inter-layer in the Ti/TiSiN coating process by Bushroa et al. [19]. The method was used to find optimal deposition parameters, such as substrate temperature, and oxygen and argon partial pressure, for the deposition of sputtered ZnO:Ga [20]. In a like manner, study [21] is related to the optimization of deposition parameters for sputtered Sm-Co films using the design of experiments with a Taguchi-fractional factorial, L8 ( $2^{4-1}$ ) design. Thus, the Taguchi method can determine the effects of the input factors on output/responses and properties of the product with the least number of experiments. To obtain the desired properties, Taguchi design, which is a statistical and mathematical method, can be used since it is an easy, reliable, cost- and time-effective method as opposed to the "one factor at a time" method. Hence, the Taguchi method can be an important tool to investigate the effect of deposition parameters, i.e., Fe deposition rates (0.02, 0.07, and 0.12 nm/s), Al deposition rates (0.03, 0.04, and 0.05 nm/s), and Fe layer thicknesses (5, 15, and 25 nm).

It should be noted that in this study most of the deposition parameters and all values of the levels, as well as the method, are different from those used in our previous work [13]. Therefore, under the study with the Taguchi method,  $M_s$  of Fe/Al MTFs was referred to, and the response and the deposition factors were analysed to obtain the improved  $M_s$  value for the films. As far as we know, the current study presents the very first process of finding the best deposition factors to obtain the improved  $M_s$  of the Fe/Al MTFs deposited by dual-target dc magnetron sputtering, using the Taguchi method supported by response surface methodology (RSM), analysis of variance (ANOVA), and regression analysis. The L9 factor design of the Taguchi method was used to find the improved  $M_s$  value with a desired

L9 standard OA.

Experimental run order	Deposition factors		
	A	B	C
1	1	1	1
2	1	2	2
3	1	3	3
4	2	2	3
5	2	3	1
6	2	1	2
7	3	3	2
8	3	1	3
9	3	2	1

TABLE II

combination of deposition factors with three levels. ANOVA was applied to see what the significance of each factor on  $M_s$  was, and RSM was applied to see the interactions of the factors. Also, regression analysis was performed to predict the measured value of  $M_s$ . For regression analysis, the equations of  $M_s$  were obtained based on the deposition parameters. Finally, the reliability of the results was tested by the verification experiment, and  $M_s$  was found to have improved to 1649.0 emu/cm<sup>3</sup> in the prescribed recipe and is expected to have potential use in magnetic applications.

## 2. Experimental methods

### 2.1. Deposition process and measurement methods

Fe/Al MTFs were produced using a dual-target sputtering system (Mantis, QPREP500). The dual-target sputtering system permits the desired independent layer for multilayer production. Iron (Kurt J. Lesker Company, 99.99%) and aluminium (Kurt J. Lesker Company, 99.99%) targets have thicknesses of 1 mm and 2 mm, respectively, and the diameter is 50.8 mm. A commercially available acetate layer was used as a substrate. Before the production process, the substrate was prepared as in [22]. After the cleaning process was completed, the substrate was placed in the chamber opposite the targets at each deposition. The deposition was carried out under an argon atmosphere of 40 sccm in the vacuum chamber. The desired thickness was achieved on an acetate substrate rotated at 20 rpm and was monitored using a quartz crystal thickness monitor.

Fe deposition rates (deposition factor A) were 0.02, 0.07, and 0.12 nm/s, and Al deposition rates (deposition factor B) were 0.03, 0.04, and 0.05 nm/s. Fe layer thicknesses (deposition factor C) were 5, 15, and 25 nm and symbolized as X[Fe(5 nm)/Al(5 nm)], X[Fe(15 nm)/Al(5 nm)], and X[Fe(25 nm)/Al(5 nm)], respectively. The bilayer number (X) was set to 12, 6, and 4,

TABLE III

 The experimental recipes and  $M_s$  values with S/N ratios.

Experimental run order	Factors			Experimental results	
	A — Fe deposition rate [nm/s]	B — Al deposition rate [nm/s]	C — Fe layer thickness [nm]	Saturation magnetisation, $M_s$ [emu/cm <sup>3</sup> ]	S/N ratio for $M_s$ [dB]
1	0.02	0.02	5	767.2	57.7
2	0.02	0.03	15	1196.6	61.6
3	0.02	0.04	25	1326.6	62.5
4	0.07	0.02	15	1455.1	63.3
5	0.07	0.03	25	1574.7	63.9
6	0.07	0.04	5	833.8	58.4
7	0.12	0.02	25	1521.7	63.7
8	0.12	0.03	5	995.6	60.0
9	0.12	0.04	15	1599.2	64.1

Initial combination = A3B3C2

respectively, to obtain the total thicknesses of 120 nm. Al thickness was fixed at 5 nm. The films were deposited according to the run list obtained from the Taguchi method and kept in a desiccator. The representation of deposition factors and levels can be seen in Table I. The 9-run experimental design is also displayed in Tables II and III.

Magnetisation measurements were done by using a vibrating sample magnetometer (VSM) (ADE Technologies EV9) at room temperature. A magnetic field of  $\pm 10$  kOe was used to obtain  $M_s$  values from the magnetic hysteresis loops. Elemental analysis of the film was carried out with energy-dispersive X-ray spectroscopy (EDX) (AMETEK EDAX Element). The film crystal structures were investigated with a Bruker X-ray diffractometer (XRD). The scan of the films was carried out with Cu  $K_\alpha$  radiation ( $\lambda = 1.54 \text{ \AA}$ ) between  $35^\circ$  and  $90^\circ$ . Surface morphology analysis was made with a scanning electron microscope (SEM) (Hitachi SU5000). Taguchi method analyses, RSM and regression analysis for the films have been done with a trial version of Minitab 18.

## 2.2. Taguchi design

In a full factorial design, the number of experiments significantly increases with the increase of process factors. As an alternative, the Taguchi method is a simple and reliable procedure, which is applied to find the best process factors with the least number of experiments, and thus in the shortest time, compared to the classical full factorial design approach [23–26]. In the Taguchi method, the loss function was used [27] to calculate the relationship between the experimental and desired values. This loss function was transferred into a signal-to-noise (S/N) ratio [28]. Usually, the S/N ratio analysis has three levels, namely, the higher-the-better (HB), the lower-the-better (LB) and the nominal-the-better (NB). The S/N ratio for each level of pro-

cess factors was calculated based on the S/N analysis. Whichever S/N ratio is used, the highest S/N ratio gives the best result. In our study, a higher  $M_s$  value is an indication of better performance. Thus, the S/N ratios for HB (maximise) characteristics were used for the improved  $M_s$  value and computed as follows [28]

$$[S/N]_{\text{HB}} = -10 \log \left( \frac{1}{n} \sum_{i=1}^n \frac{1}{y_i^2} \right), \quad (1)$$

where  $n$  is the number of observations and  $y$  is the observed data. The ratios S/N of each of the  $M_s$  values,  $y$ , were computed for  $n = 1$ , shown in Table III. Also, L9 orthogonal arrays (OA) were used to find optimal values of the objective function in manufacturing processes with a minimum number of experiments. Taguchi method was used to analyse deposition factors A, B, and C.

## 2.3. ANOVA

ANOVA is used to find whether the influence of the process factors is important or not [23, 29]. In this study, ANOVA was used to analyse the deposition factors A, B, and C. The F-ratio and the contribution percentage of the deposition factors of S/N ratios were computed.

## 2.4. RSM

The RSM model is based on the response surface analysis of the design matrix results [30–32]. In our study, RSM was applied to find the interactions between the factors to improve  $M_s$  since interactions of deposition factors cannot be determined using the Taguchi design. The significance of each factor in the response is also determined. Also, the results obtained from the RSM can precisely estimate  $M_s$  without further performing the experimental runs for the deposition factors A, B, and C.

## 2.5. Regression analysis

Regression analysis can be applied to analyse the relationship between an output/response factor and one or more input/process factors [33]. In this study, the output/response deposition factor is  $M_s$ , and the input/process deposition factors are A, B, and C. For the quadratic regression model, the first and second order and their interaction analysis of the responses were obtained for all process factors.

## 3. Results and discussion

### 3.1. Assessment of Taguchi method

#### 3.1.1. Levels and orthogonal array

The influence of deposition factors on  $M_s$  values of Fe/Al MTFs was studied using the Taguchi method. The deposition factors with three levels (low, medium and high), i.e., A — Fe deposition rate, B — Al deposition rate, and C — Fe layer thickness, were selected from the previous trials and are shown in Table I.

To choose an appropriate OA for the deposition factors described in Table I, Taguchi L9 standard OA was selected and shown in Table II. In the table, nine combinations of deposition factors were created. Film depositions were performed according to these designs for each combination of the deposition factors. Figure 1 presents the hysteresis loops of all films measured with the VSM that are sputtered to the designs given in the L9 array in Table II. From the loops of the runs,  $M_s$  values were obtained and are presented in Table III. Coercivities of the films were also determined and found to be  $\sim 110$  Oe for all films.

#### 3.1.2. Analysis of the S/N ratio

The quality characteristics of deposition factors were determined by the S/N ratios. The S/N ratios were computed using the “larger is the better” condition, i.e., (1), and are presented in Table III. The initial highest  $M_s$  combination was found to be A3B3C2 (see Table III).

Since the experimental design was orthogonal, the effects of deposition factors were divided in terms of the S/N ratio. The highest levels of the mean S/N ratio of all factors are given in Table 4. Also, the average S/N ratios corresponding to each level of deposition factor for  $M_s$  values are given in Fig. 2. There, the highest condition corresponds to the maximisation of  $M_s$  value. Thus, the highest levels were determined as A3 (Fe deposition rate — 0.12 nm/s), B2 (Al deposition rate — 0.03 nm/s), and C3 (Fe layer thickness — 25 nm). The significance of each deposition factors can be determined from the delta values of the S/N ratio analysis. The difference between the lowest and highest values (delta) of each deposition factor can also be seen in Fig. 2. For the delta values, the most significant

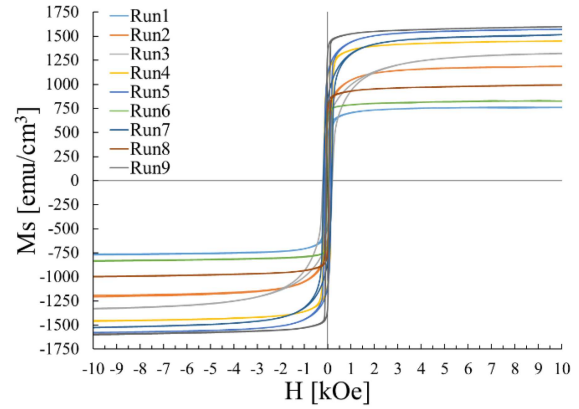


Fig. 1. Hysteresis loops of the films sputtered according to the runs displayed in Table II.

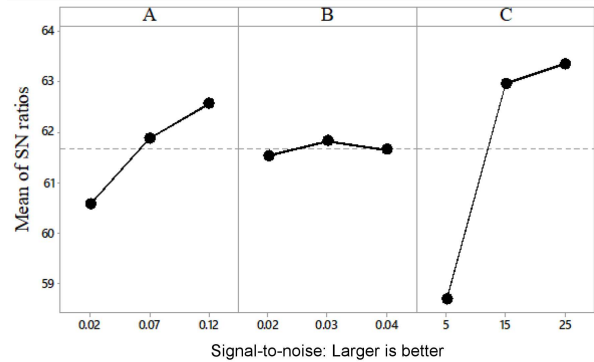


Fig. 2. Effects of deposition factors on average S/N ratios. The dashed line represents the averages of the mean of S/N ratios.

deposition factor is C (Fe layer thickness), with the highest delta value. The second most effective factor A (Fe deposition rate), while B (Al deposition rate) is the least effective one. The order of effectiveness is given in Table IV as “Rank”.

### 3.2. ANOVA results

The F-ratio and contribution percentage of the deposition factors were computed according to the ANOVA method to determine the extent to which the response is influenced by the individual deposition factors. Table V shows the calculated ANOVA results with 95% confidence. As can be seen in the table, two deposition factors, A and C, have influences on  $M_s$  value. The F-ratio of deposition factor C is the most important contribution, with a value of 26.66, followed by the F-ratio of deposition factor A, which is 4.70. No F-ratio of deposition factor B was observed. As for percentage contributions, the most influential deposition factor on  $M_s$  is factor C with a contribution rate of 87.41%, followed by deposition factor A, the percentage contribution of which is 12.59%. No contribution of deposition factor B was observed. The error contribution to the

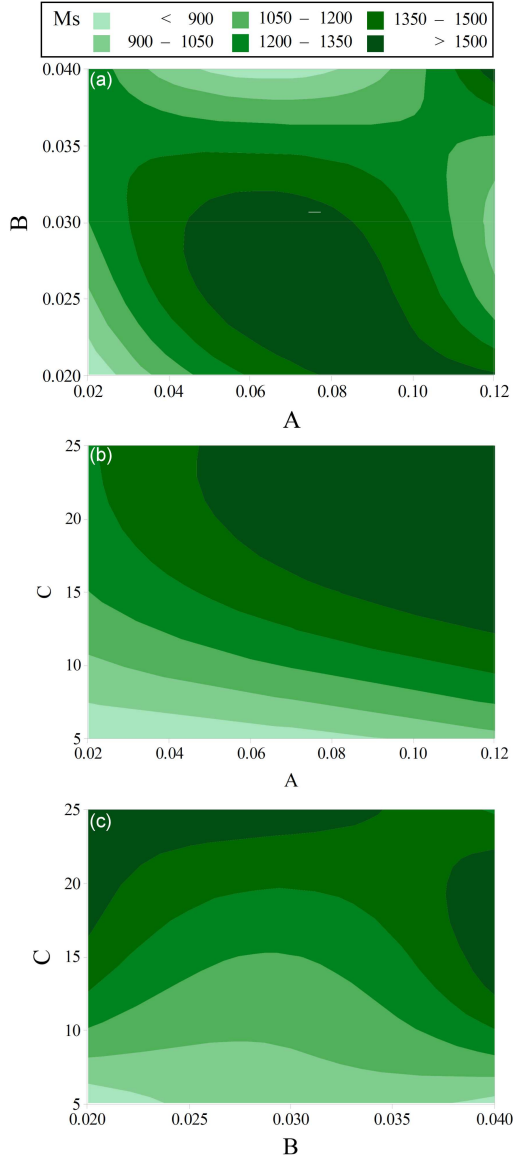


Fig. 3. Response counter plots of two variables on  $M_s$  values: (a) A and B; (b) A and C; (c) B and C.

system was zero percent. These results verify the delta and rank order of the factors determined by the S/N ratios.

### 3.3. Deposition factors with RSM

The changes in  $M_s$  values against deposition factors generated in the RSM experimental study are presented in Fig. 3a–c. The interaction can be determined according to the figure in which  $M_s$  values were plotted against two factors. In Fig. 3a, the highest  $M_s$  is observed for medium and high values of factor A and low and medium values of factor B. Besides, the highest levels for both factor A and B give a high  $M_s$  value according to Fig. 3a. As shown in Fig. 3b, the highest  $M_s$  can be obtained at higher values of both factor A and C. Figure 3c

TABLE IV

Deposition factors for mean S/N ratios [dB]. Underlined values show the levels for the highest  $M_s$  obtained from the experimental study.

Levels	Factors		
	A	B	C
Level 1	60.57	61.53	58.69
Level 2	61.87	<u>61.82</u>	62.96
Level 3	<u>62.56</u>	61.65	<u>63.35</u>
Delta	1.99	0.29	4.65
Rank	2	3	1

shows two combinations to obtain high  $M_s$ ; one is for low and medium values of factor B and higher values of factor C, the other is for higher values of factor B and medium values of factor C. It can be concluded from Fig. 3a and c that factor B has little effect on  $M_s$  of the films. The figures verify the results of the Taguchi method, which is used to determine the influence of each independent factor on  $M_s$  value (Table IV and Fig. 2). Also, ANOVA showed the significance of each factor for  $M_s$  (Table V). Depending on the analysis, there were significant changes in the effect of factors C and A on  $M_s$  values. According to the differences in the factors, the highest  $M_s$  was obtained at the combination A3B2C3. The most significant factor affecting  $M_s$  value was factor C. The optimal conditions for the highest  $M_s$  value can be derived by RSM without performing further experimental runs. The RSM results verify the effect of each individual deposition factor on  $M_s$  value obtained with Taguchi and ANOVA statistical analysis.

### 3.4. Taguchi method verification experiment

For the confirmation of the results under the best deposition conditions, the verification experiment was applied using the highest  $M_s$  setting of the deposition factors, i.e., A3B2C3 (A — 0.12 nm/s, B — 0.03 nm/s, and C — 25 nm). The film was deposited according to this recipe, and the saturation magnetisation was found to be  $M_{s, \text{exp}} = 1649.0 \text{ emu/cm}^3$ . The film magnetic hysteresis loop is given in Fig. 4. Coercivity of the film was 110 Oe, which is close to the coercivity of the recipes of the Taguchi method given in Table III and Fig. 1 ( $\sim 110 \text{ Oe}$ ). The films showed semi-hard magnetic properties.

### 3.5. Structural characterizations of the film sputtered according to the A3B2C3 recipe

According to the EDX measurements, the elemental analysis showed that Fe/Al MTF consists of 45% Fe and 55% Al with the best recipe of A3B2C3. Local EDX measurements were also

Results of ANOVA for  $M_s$ . Underlined values show the factor for the highest  $M_s$  value.

TABLE V

Variance source	Degree of freedom (DOF)	Sum of squares (SS)	Mean square (MS)	F-ratio	Contribution rate [%]
A	2	119440	59720	4.70	12.59
B	2	91	46	0.0	0.00
<u>C</u>	<u>2</u>	<u>678007</u>	<u>339004</u>	<u>26.66</u>	<u>87.41</u>
Error	2	25430	12715	–	0.00
Total	8	47.2742	–	–	100.00

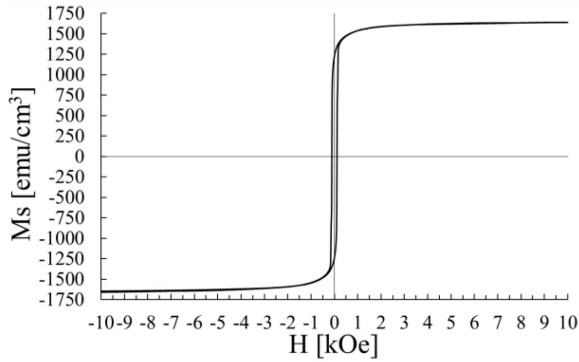


Fig. 4. Magnetization loop of the film deposited according to the optimum recipe.

made through the surface of the film, and it was confirmed that the film has homogenous composition. Figure 5a displays the XRD pattern of the film obtained at  $2\theta = 35-90^\circ$ . Two peaks appear at  $2\theta \approx 44^\circ$  and  $2\theta \approx 64^\circ$  in the pattern. The peak around  $44^\circ$  can be considered Al (200) face-centred cubic (fcc) + Fe (110) body-centred cubic (bcc) for Fe/Al MTF. The peak at  $2\theta \approx 64^\circ$  was determined as Fe (200) bcc peak. According to the result obtained from the XRD analysis, it can be concluded that the film crystalline phase is a mixture of fcc and bcc structure. SEM images with 20.000 $\times$  and 45.000 $\times$  magnifications for produced Fe/Al films are presented in Fig. 5b and c. In Fig. 5b, there are some slight oblique lines/structures extending from the upper side to the bottom side of the SEM image. By examining Fig. 5c, it is observed that the film surface has some grains with dimensions up to  $\sim 150$  nm. The local EDX measurements obtained on the grains indicated almost the same content of the film.

### 3.6. Prediction of the improved saturation magnetisation

Using the initial and highest combinations of deposition factors in the trial version of Minitab,  $M_s$  values were predicted as  $M_{s,ini} = 1540.2$  emu/cm<sup>3</sup> and  $M_{s,pred} = 1597.6$  emu/cm<sup>3</sup>, respectively.

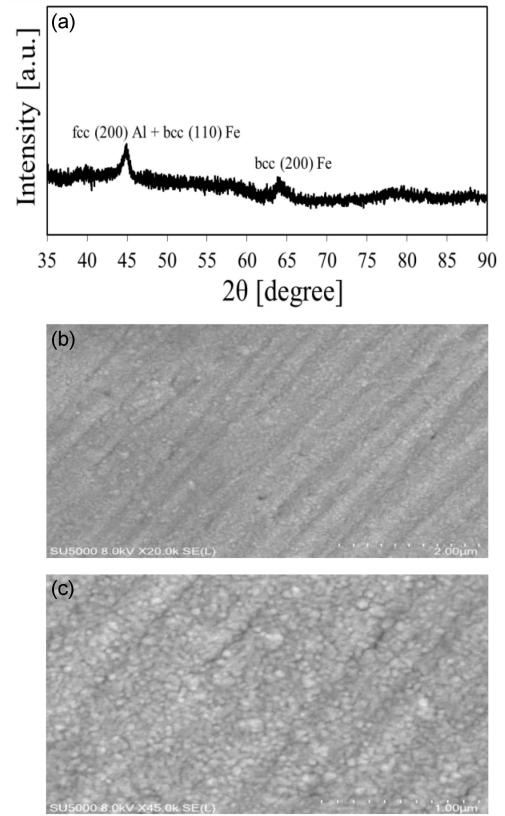


Fig. 5. (a) XRD structural pattern of the Fe/Al film deposited under optimum deposition conditions and SEM images with different magnifications, (b) 20.000 $\times$  and (c) 45.000 $\times$ , for sputtered Fe/Al film.

### 3.7. Regression analyses of saturation magnetisation

Quadratic regression analysis was imposed to derive the predictive equations of the  $M_s$  value. The equation of  $M_s$  was obtained based only on the deposition factors and their interactions. The regression model was also used to generate the predictive equation. The analysis includes all factors, quadratic terms and their interactions. The quadratic model is

$$(R^2 = 100\%R^2(\text{adj}) = 100\%). \quad (2)$$



TABLE VI

The error percentage of Taguchi experimental and the predicted results to Taguchi method and quadratic regression equation

Levels	Taguchi	Taguchi		Quadratic	
	exper. results	prediction		regression prediction	
	$M_s$ [emu/cm <sup>3</sup> ]	$M_s$ [emu/cm <sup>3</sup> ]	Error [%]	$M_s$ [emu/cm <sup>3</sup> ]	Error [%]
A3B3C2 (Initial combination)	1599.2	1540.2	3.69	1599.3	0.01
A3B2C3 (highest confirmation)	1649.0	1597.6	3.12	1649.0	0.00

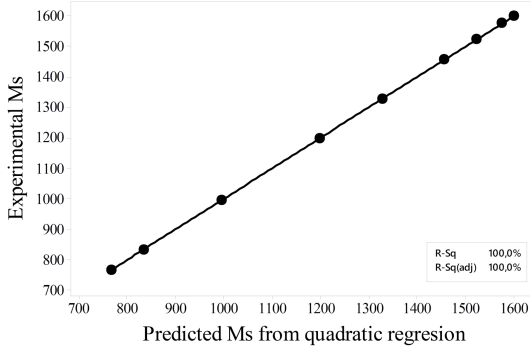


Fig. 6. Relationships between quadratic factor regression and experimental results for  $M_s$ .

The measured and the estimated responses that were computed with (2) are presented in Fig. 6. Very good statistical performance with both  $R^2$  and  $R^2(\text{adj})$  values of 100% was obtained. Therefore, the regression equation can much more successfully obtain the predicted  $M_s$ .

### 3.8. Comparison of experimental and predicted values

Experimental results from the Taguchi method and predicted values from the quadratic regression equation (see (2)) at initial and highest levels are displayed in Table VI. Error values must be less than 20% for reliable statistical analyses [28]. As can be seen in Table VI, experimental and predicted  $M_s$  values are very close to each other. The calculated error percentages for  $M_s$  values are well within the acceptable levels. Therefore, the results obtained from the confirmation test reflect a successful improvement of  $M_s$ . Error percentages of the regression equation were the smallest (0.01 and 0.00 %), followed by those of the Taguchi method (3.69 and 3.12%). It has been shown that the quadratic regression equation can be much more successfully applied to obtain the predicted  $M_s$  values.

## 4. Conclusions

Under In our study, the Taguchi method was found to be very successful in finding the proper deposition factors in order to improve the value

of  $M_s$  of Fe/Al MTFs sputtered by a dual-target dc magnetron. Using the “larger is the better” approach based on the S/N ratio from the method, the improved  $M_s$  value under best deposition conditions was observed at A3B2C3, i.e., deposition factor A is 0.12 nm/s, deposition factor B is 0.03 nm/s, and deposition factor C is 25 nm. From this recipe, it was experimentally observed that  $M_s$  of Fe/Al MTFs is  $M_{s, \text{exp}} = 1649.0 \text{ emu/cm}^3$ , which is an improvement from the highest initial run,  $M_{s, \text{ini}} = 1540.2 \text{ emu/cm}^3$ , within the prescribed limit. A predicted value of  $M_s$  with a 95% confidence level was  $1597.6 \text{ emu/cm}^3$ . Therefore, it can be seen that the Taguchi method also has good results in  $M_s$  estimation of Fe/Al MTFs. To the crystalline structure analysis, the XRD pattern of the film has Al (200) fcc + Fe (110) bcc peak and Fe (200) bcc peak.

According to the results of ANOVA for  $M_s$ , the most significant deposition factor was factor C, which had a percentage contribution of 87.41%. It is followed by the deposition factor A, which had around 12.59% contribution. No effect was observed of deposition factor B. According to the effect of each factor, ANOVA results were found to be the same as the order of S/N ratios of  $M_s$ .

In RSM, interactions were created depending on the highest, medium, and lowest levels of the deposition factors (A, B, and C). Depending on the differences in the factors, the highest  $M_s$  was obtained at the combination A3B2C3. The most significant factor affecting the  $M_s$  value was deposition factor C. The optimal conditions for the highest  $M_s$  value can be derived by the RSM without performing further experimental runs. The RSM results verify the effect of each individual deposition factor on the  $M_s$  value obtained with the Taguchi method and the significance of each deposition factor on  $M_s$  values with ANOVA.

The quadratic regression model demonstrated the best relationship between the measured and quadratic predicted values for  $M_s$  with the confidence intervals of  $R^2 = 100$  and  $R^2(\text{adj}) = 100\%$ . This means that the predicted values and measured values fit each other.

Confirmation and predicted test results from the Taguchi method and regression equation at initial and highest levels are compared. The values are very close to each other. The error percentage of the quadratic predicted result was the smallest one.

This is followed by the Taguchi method. It has been observed that quadratic regression equations can be quite successfully applied and predict  $M_s$  values of Fe/Al MTFs.

As the Taguchi method supported by RSM, ANOVA, and regression analysis tools performs well in improving  $M_s$  values of Fe/Al MTFs model, it can also be applied to other deposition systems of multilayers for potential magnetic applications.

### Acknowledgments

This work was supported by Balikesir University Research Grant no. BAP 2021/054. The authors would like to thank State Planning Organization, Turkiye under Grant no. 2005K120170 for the VSM system and Karamanoglu Mehmetbey University, Turkiye for XRD, SEM, and EDX measurements.

### References

- [1] Y. Mu, P. Li, Y.Wen, S.Yu, Y. Wang, L. Bian, T. Han, X. Ji, *J. Magn. Magn. Mater.* **533**, 168025 (2021).
- [2] Q.H. Hao, H.W. Dai, M.H. Cai, X.D. Chen, Y.T. Xing, H.J. Chen, T.Y. Zhai, X. Wang, J.B. Han, *Adv. Electron. Mater.* **8**, 2200164 (2022).
- [3] S.P. Dalawai, S. Kumar, M.A. Saad Aly, M.Z.H. Khan, R. Xing, P.N. Vasambekar, S. Liu, *J. Mater. Sci. Mater. Electron.* **30**, 7752 (2019).
- [4] N. Rajasekaran, S. Mohan, *Crit. Rev. Solid State Mater. Sci.* **37**, 158 (2012).
- [5] R.R. Kumar, P. Gowrisankar, V. Balaparakash, S. Sudha, E.I. Manimaran, *J. Mater. Sci. Mater. Electron.* **29**, 11591 (2018).
- [6] S.M. Suturin, P.A. Dvortsova, M.V. Baidakova, M.S. Dunaevskiy, B.B. Krichevstov, *J. Magn. Magn. Mater.* **557**, 169467 (2022).
- [7] B. Sharma, A. Sharma, *Appl. Surf. Sci.* **567**, 150724 (2021).
- [8] S. Çölmekçi, A.Karpuz, H. Köçkar, *J. Magn. Magn. Mater.* **478**, 48 (2019).
- [9] M. Zhang, C. Deng, *J. Mater. Sci. Mater. Electron.* **32**, 4949 (2021).
- [10] Y. Satake, K. Fujiwara, J. Shiogai, T. Seki, A. Tsukazaki, *Sci. Rep.* **9**, 3282 (2019).
- [11] W. Zhou, Y. Sakuraba, *Appl. Phys. Express* **13**, 043001 (2020).
- [12] J. Gardy, A. Osatiashtiani, O. Céspedes, A. Hassanpour, X. Lai, A.F. Lee, K. Wilson, A. Rehan, *Appl. Catal. B Environ.* **234**, 268 (2018).
- [13] A. Karpuz, H. Köçkar, S. Çölmekçi, M. Uçkun, *J. Superconduct. Novel Magn.* **33**, 463 (2020).
- [14] R. Brajpuriya, *J. Appl. Phys.* **107**, 083914 (2010).
- [15] S. Kamaruddin, Z.A. Khan, S.H. Foong, *Int. J. Eng. Technol.* **2**, 574 (2010).
- [16] S.R. Rama, G. Padmanabhan, *Int. J. Eng. Res. Appl.* **2**, 192 (2012).
- [17] R. Adikesavulu, B. Sreenivasulu, B. Sreenivasulu, *Int. J. Innov. Eng. Res. Technol.* **1**, 1 (2014).
- [18] R. Manohara, A. Harinath, *Int. J. Trend Sci. Res. Dev.* **3**, 1052 (2019).
- [19] A.R. Bushroa, H.H. Masjuki, M.R. Muhamad, *Int. J. Mech. Mater. Eng.* **6**, 140 (2011).
- [20] X. Bie, J. Lu, Y. Wang, L. Gong, Q. Ma, Z. Ye, *Appl. Surf. Sci.* **257**, 6125 (2011).
- [21] G.V. Ramana, P. Saravanan, S.V. Kammat, Y. Aparna, *Appl. Surf. Sci.* **261**, 110 (2012).
- [22] A. Karpuz, S. Colmekci, H. Kockar, H. Kuru, M. Uckun, *Z. Naturforsch. A* **73**, 85 (2018).
- [23] P.J. Ross, *Taguchi Techniques for Quality Engineering Loss Function, Orthogonal Experiments Parameter and Tolerance Design*, McGraw-Hill International Book Company, New York 1989.
- [24] G. Taguchi, *Introduction to Quality Engineering*, Asian Productivity Organization (APO), Tokyo 1990.
- [25] D. Fratila, C. Caizar, *J. Clean. Prod.* **19**, 640 (2011).
- [26] T.V. Sibalija, V.D. Majstorovic, *J. Intell. Manuf.* **23**, 1511 (2012).
- [27] S.H. Park, *Robust Design and Analysis for Quality Engineering*, Chapman & Hall, London 1996.
- [28] N. Mandal, B. Doloi, B. Mondal, R. Das, *Measurement* **44**, 2149 (2011).
- [29] K. R. Roy, *A primer on Taguchi Method*, Van Nostrand Reinhold, New York 1990.
- [30] J. Grum, J.M. Slabe, *J. Mater. Process. Technol.* **155**, 2026 (2004).
- [31] V.I. Vitanov, N. Javaid, D.J. Stephenson, *Surf. Coat. Technol.* **204**, 3501 (2010).
- [32] B. Bhattacharya, S.K. Sorkhel, *J. Mater. Process. Technol.* **86**, 200 (1999).
- [33] M.H. Cetin, B. Ozelik, E. Kuram, E. Demirbas, *J. Clean. Prod.* **19**, 2049 (2011).